# Polymorphs and co-crystals of haloprogin: an antifungal agent†

Michele Baldrighi,[a] Davide Bartesaghi,[a] Gabriella Cavallo,[a] Michele R. Chierotti,[b] Roberto Gobetto,[b] Pierangelo Metrangolo,*[a] Tullio Pilati,[a] Giuseppe Resnati*[a] and Giancarlo Terraneo*[a]

Received 19th February 2014,
Accepted 16th April 2014

## Introduction

Polymorph screening and co-crystal formation are useful strategies to find new solid forms of active pharmaceutical ingredients (APIs), in order to alter or improve their physical properties without changing their chemical identities or biological activities.[1] Most commonly, APIs have hydrogen bonding donor and acceptor groups that are involved in the binding of the co-crystal former (CCF), *e.g.*, carboxylic acids and aromatic nitrogen atoms have been proven particularly reliable moieties in the hydrogen bonding (HB) driven formation of API-CCF adducts.[2] On the other hand, the design of pharmaceutical co-crystals involving APIs devoid of strong hydrogen bond donor sites is quite challenging.

Halogen atoms are frequently present in drug molecules and we have considered that they can be used to drive the formation of pharmaceutical co-crystals if halogen bonding[3] (XB) is used. Recently we demonstrated that the iodoalkyne moiety of an API can be successfully used to prepare halogen-bonded co-crystals with improved physicochemical properties.[4] In this paper we describe a further case where the same moiety drives the formation of co-crystals with neutral and anionic partners. More important, we describe how the iodoalkyne moiety can play an active role in the formation of different polymorphs of an API.

Haloprogin **1** (1,2,4-trichloro-5-[(3-iodoprop-2-yn-1-yl)oxy]benzene) is the API of antimycotic topical drugs with brand names Halotex®, Mycanden®, Mycilan® and Polik® (Scheme 1).[5] No structures involving **1** are reported in the Cambridge Structural Database (CSD),[6] consistent with the fact that it may represent a difficult challenge if a standard approach for polymorph and co-crystal formation is pursued since it does not contain any of the functional groups typically required for a HB-based strategy.[1,2]

On the other hand, an iodine atom bound to a sp-hybridised carbon atom displays a particularly anisotropic distribution of its electron density.[7] A region of remarkably positive electrostatic potential, the so-called positive σ-hole,[8] is present on the outermost surface of the iodine atom and along the extension of the C–I covalent bond. This specific feature makes the iodoalkyne moiety a very good XB donor site.[9,10] We have reasoned that the presence in **1** of one efficient XB donor site along with the absence of strong HB donor sites represents a unique opportunity to explore the

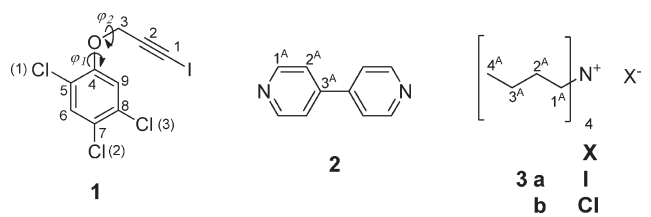


**Scheme 1** Molecular structures of haloprogin and of the used CCFs. The used atom labels are indicated for all structures. Torsion angles $\varphi_1$ and $\varphi_2$ are indicated with curved arrows.

[a] *NFMLab-Laboratory of Nanostructured Fluorinated Materials (NFMLab), Department of Chemistry, Materials, and Chemical Engineering "Giulio Natta", Politecnico di Milano, Via L. Mancinelli 7, 20131 Milan, Italy. E-mail: pierangelo.metrangolo@polimi.it, giuseppe.resnati@polimi.it, giancarlo.terraneo@polimi.it*

[b] *Department of Chemistry, Università di Torino, Via P. Giuria 7, 10125 Torino, Italy* † Electronic supplementary information (ESI) available: Synthetic procedures, DSC plots, FTIR spectra, powder XRD plots, and details of the CSD search. CCDC 986300–986305

obtainment of new co-crystals based on XB. In addition, the presence in **1** of multiple electron donor sites that may be involved in XB, *e.g.*, the chlorine atoms, the oxygen atom, and the π electrons, may favour the obtainment of different polymorphs and allows for a quite rich structural landscape for the pure API.

Three polymorphs **1a**, **1b**, and **1c** of haloprogin are described here. As far as co-crystals of **1** are concerned, we have obtained the neutral co-crystal **4** with 4,4′-bipyridine (**2**) and two ionic co-crystals **5a** and **5b** with tetra-*n*-butylammonium iodide (**3a**) and chloride (**3b**).[11] The studied CCFs were chosen in order to cover both neutral and anionic electron density donor sites, which are both well represented in the FDA-GRAS[12] (Food and Drug Administration-Generally Recognized As Safe) list. All obtained solid forms of **1** (polymorphs and co-crystals) were fully characterized by using various analytical techniques, such as single crystal and powder X-ray diffraction analyses, FTIR, differential scanning calorimetry (DSC), and solid state (SS) NMR.

## Experimental section

### Materials

Solvents and reagents were purchased from Sigma Aldrich at high purity grade and used without further purification. Haloprogin was synthesized in two steps according to the procedure reported by Fellig *et al.*[13] (see ESI†). Solution NMR spectra were collected using a Bruker AV400 spectrometer. Single crystals of polymorphs **1a** and **1b** were obtained by slow evaporation methods. Single crystals of polymorphs **1b** and **1c** were obtained *via* both slow evaporation and sublimation. Co-crystals of **4** were obtained by slow evaporation methods. Mechanochemical synthesis of **5a** and **5b** was performed using a Retsch MM400 ball mill with 5.0 mL vessels, operating at 30 Hz. Corresponding single crystals were obtained by seeding quasi-saturated solutions of **1** and **3a** or **3b**, respectively, (in the appropriate molar ratio) with the powders obtained from ball milling experiments.

**Vibrational spectroscopy.** IR spectra were collected using a Nicolet Nexus FT-IR spectrometer equipped with a Smart Endurance ATR device and analysed using the Omnic software version 7.3. Peak values are given in wavenumbers ($cm^{-1}$) upon automatic assignment.

**Thermal analysis.** Melting points were collected using a Linkam Hot-Stage microscopy apparatus. Thermal analysis was performed using a Mettler Toledo DSC 823e differential scanning calorimeter.

**X-ray crystallography.** A Bruker AXS D8 powder diffractometer was used for all X-ray powder (XRPD) measurements with experimental parameters as follows: Cu-Kα radiation ($\lambda$ = 1.54056 Å), scanning interval 4–40° at 2$\theta$, step size 0.016°, exposure time 1.5 s per step. Single crystal X-ray diffraction (XRD) data were collected using a Bruker AXS KAPPA-APEX II CCD diffractometer with Mo-Kα radiation ($\lambda$ = 0.71073 Å). Data integration and reduction were performed using SaintPlus 6.01.[14] Absorption correction was performed with a multi-scan method implemented in SADABS.[15] Space groups were determined using XPREP implemented in the APEX II suite.[16] Structures were solved using SHELXS-97 (direct methods) and refined using SHELXL-97[17] (full-matrix least-squares on $F^2$) contained in the APEX II and WinGX version 1.80.01 software packages.[18] All non-hydrogen atoms were refined anisotropically. Hydrogen atoms were placed in geometrically calculated positions and included in the refinement process using a riding model with isotropic thermal parameters. Analyses of crystal data and pictures were performed with Mercury 3.1.[19] Crystal data are reported in Table 1.

**Solid state NMR.** SSNMR measurements were performed using a Bruker AVANCE II 400 instrument operating at 400.23, 100.65 and 40.55 MHz for $^1$H, $^{13}$C and $^{15}$N NMR, respectively. $^{13}$C and $^{15}$N CPMAS spectra were recorded at room temperature with a spinning speed of 12 ($^{13}$C) or 9 kHz ($^{15}$N). Cylindrical 4 mm o.d. zirconia rotors with a sample volume of 80 μL were employed. A ramp cross-polarization pulse sequence was used with a contact time of 5 ms, a $^1$H 90° pulse of 3.30 μs, recycle delays of 10–40 s, and 512–4096 ($^{13}$C) or 1400–1600 ($^{15}$N) transients. The two pulse phase modulation (TPPM) decoupling scheme was used with a frequency field of 75 kHz. Spectral editing experiments were performed by using a CPPISPI pulse sequence with a polarization inversion time of 65–85 μs in order to obtain positive $CH_3$ and $C_q$, null CH, and negative $CH_2$. $^{13}$C and $^{15}$N scales were calibrated with glycine ($^{13}$C methylene signal at 43.86 ppm) and $(NH_4)_2SO_4$ ($^{15}$N signal at $\delta$ = 355.8 ppm with respect to $CH_3NO_2$) as external standards. $^{13}$C and $^{15}$N chemical shift assignments for pure reagents and for the co-crystals are in the SI. Atom labels used in SSNMR studies are reported in Scheme 1. Spectral editing techniques were useful for unambiguous assignments. All $^{13}$C and $^{15}$N chemical shifts with assignments are reported in Table S1 in the ESI.†

**Conformational and computational analysis.** Conformational comparison was performed overlapping the aromatic portions of the three polymorphs of **1**. Energy calculations were performed at the MP2/6-311+G(d,p) level of theory of the Spartan Software.[20] The molecular geometry obtained by the X-ray studies was used for these analyses.

### Preparation of polymorphs and co-crystals

**Synthesis of polymorph 1a.** In a 2.5 mL glass vial, 10 mg of **1** (0.027 mmol) were dissolved in 1.5 mL of chloroform. The open vial was left in the hood at room temperature and after 17 hours clear colourless octahedral crystals of **1a** were found at the bottom of the vial. M.p.: 111 °C. FTIR (selected bands): 2187, 1581, 1472, 1453, 1232, 1077, 1028, 866, 724, 681 $cm^{-1}$.

**Syntheses of polymorphs 1b and 1c.** In a 2.5 mL glass vial, 11.7 mg of **1** (0.032 mmol) were dissolved in 1.0 mL of chloroform, then a solution of sodium acetate (2.9 mg, 0.032 mmol) in methanol (1.0 mL) was stratified on top of the solution of **1**. The vial was capped and the solvents slowly evaporated through a needle in the cap.

Table 1 Crystallographic data of polymorphs **1a–c** and co-crystals **4** and **5a, b**

| | 1a | 1b | 1c | 4 | 5a | 5b |
|---|---|---|---|---|---|---|
| Chemical formula | $C_9H_4Cl_3IO$ | $C_9H_4Cl_3IO$ | $C_9H_4Cl_3IO$ | $C_{28}H_{16}Cl_6I_2N_2O_2$ | $C_{34}H_{44}Cl_6I_3NO_2$ | $C_{34}H_{44}Cl_7I_2NO_2$ |
| Formula weight | 361.37 | 361.37 | 361.37 | 878.93 | 1092.10 | 1000.65 |
| Temperature K | 295 | 296 | 296 | 296 | 296 | 103 |
| Crystal system | Monoclinic | Triclinic | Monoclinic | Triclinic | Orthorhombic | Orthorhombic |
| Space group | *C*2/*c* | $P\bar{1}$ | *C*2/*c* | $P\bar{1}$ | *Pbcn* | *Pbcn* |
| *a* (Å) | 22.173(2) | 4.2659(6) | 31.100(5) | 7.4865(14) | 8.9174(9) | 8.557(2) |
| *b* (Å) | 7.6870(7) | 10.4936(14) | 5.3807(7) | 13.522(3) | 15.2187(12) | 14.816(3) |
| *c* (Å) | 13.8308(13) | 13.3814(16) | 13.861(2) | 17.240(3) | 31.429(3) | 31.189(6) |
| $\alpha$ (°) | 90.00 | 108.226(12) | 90 | 67.769(9) | 90.00 | 90.00 |
| $\beta$ (°) | 109.181(4) | 93.893(12) | 107.050(5) | 81.362(9) | 90.00 | 90.00 |
| $\gamma$ (°) | 90.00 | 90.291(12) | 90 | 79.166(9) | 90.00 | 90.00 |
| Volume (Å$^3$) | 2226.5(4) | 567.43(13) | 2217.5(6) | 1580.7(5) | 4265.3(7) | 3954.2(14) |
| *Z* | 8 | 2 | 8 | 2 | 4 | 4 |
| Density (g cm$^{-3}$) | 2.156 | 2.115 | 2.159 | 1.847 | 1.701 | 1.681 |
| $\mu$ (mm$^{-1}$) | 3.588 | 3.490 | 3.572 | 2.526 | 2.603 | 2.095 |
| *F* (000) | 1360 | 340 | 1352 | 844 | 2128 | 1984 |
| ABS $T_{min}$,$T_{max}$ | 0.6548, 0.7465 | 0.5823, 0.7452 | — | 0.4510, 0.9125 | 0.3943, 0.5199 | 0.5999, 0.7458 |
| $\theta_{min,max}$ (°) | 1.94, 32.86 | 1.61, 27.75 | 2.74, 24.99 | 1.28, 32.32 | 2.59, 29.25 | 2.72, 38.01 |
| $h_{min,max}$ | −32, 25 | −5, 5 | −31, 32 | −10, 10 | −12, 12 | −13, 14 |
| $k_{min,max}$ | −10, 11 | −13, 13 | −6, 6 | −20, 16 | −20, 20 | −25, 23 |
| $l_{min,max}$ | −21, 21 | −16, 16 | −16, 9 | −24, 24 | −42, 43 | −51, 51 |
| No. of reflections | 15 765 | 13 209 | 2364 | 30 410 | 61 875 | 91 960 |
| No. unique reflections | 3779 | 2461 | 1634 | 9602 | 5811 | 10 012 |
| No of parameter | 127 | 127 | 128 | 361 | 211 | 211 |
| $R_{\_all}$, $R_{\_obs}$ | 0.0452, 0.0366 | 0.0385, 0.0314 | 0.1436, 0.1236 | 0.0546, 0.0303 | 0.0524, 0.0341 | 0.0405, 0.0267 |
| $wR_{2\_all}$, $wR_{2\_obs}$ | 0.1082, 0.1035 | 0.0785, 0.0737 | 0.2992, 0.2744 | 0.0733, 0.0633 | 0.0869, 0.0736 | 0.0537, 0.0497 |
| $\Delta\rho_{max,min}$ (e Å$^{-3}$) | −1.001, 1.126 | −0.993, 0.609 | −1.631, 4.982 | −0.482, 0.713 | −0.858, 1.013 | −1.766, 1.237 |
| G.o.F | 1.058 | 1.059 | 1.044 | 1.004 | 1.079 | 1.086 |
| CCDC | 986303 | 986304 | 986305 | 986300 | 986302 | 986301 |

After two days, needles of **1b** and a few small needles of **1c** appeared along with many crystals of **1a**. **1a**, **1b**, and **1c** were separated by visual inspection. M.p.: **1b**, 113 °C; **1c**, 91 °C; FTIR of **1b** (selected bands): 3100, 2928, 2186, 1582, 1471, 1335, 1233, 1077, 867, 725 cm$^{-1}$.

**Syntheses of polymorphs 1b and 1c by sublimation.** The crude powder **1a** was sublimated at 80 °C under a vacuum ($P$ ~ 20 mbar). After 10 hours, a mixture of **1b** and **1c** crystals was collected on a glass slide fixed to the water cooled condenser. The **1c** crystals completely transformed into polycrystalline **1a** upon standing at room temperature.

**Synthesis of 4 (haloprogin : bipyridyl, 2 : 1 ratio).** In a 10 mL glass vial 400 mg (1.106 mmol) of **1** were dissolved in 5.0 mL of dichloromethane, then a solution of 4,4′-bipyridyl (84.7 mg, 0.553 mmol) in 2 mL of dichloromethane was added. The open vial was left in the hood at room temperature. After three days, several yellowish prisms appeared at the bottom and on the walls of the vial. M.p.: 118 °C; FTIR (selected bands): 3096, 2178, 1620, 1473, 1336, 1078, 1026, 801, 723, 614 cm$^{-1}$.

**Synthesis of 5a (haloprogin : tetra *n*-butylammonium iodide, 2 : 1 ratio).** 200 mg of **1** (0.553 mmol) and 102 mg of tetra-*n*-butylammonium iodide (0.277 mmol) were ground together using a high-speed ball milling apparatus for 30 min at 30 Hz. Powders were collected and analyzed by FTIR, XRPD, and DSC. M.p.: 67 °C; FTIR (selected bands): 2957, 2872, 2180, 1585, 1473, 1377, 1240, 1077, 1033, 764 cm$^{-1}$. Single crystals were obtained by seeding a quasi-saturated solution of **1** and **3a** (2 : 1 molar ratio) in methanol with the finely ground powders obtained from the solid-state synthesis, and then allowing for the slow evaporation of the solvent at room temperature.

**Synthesis of 5b (haloprogin : tetra-*n*-butylammonium chloride, 2 : 1 ratio).** 500 mg of **1** (1.383 mmol) and 192 mg of tetra-*n*-butylammonium chloride (0.692 mmol) were ground together using a high-speed ball milling apparatus for 30 min at 30 Hz. The resulting powder was collected and analyzed by FTIR, XRPD, and DSC. M.p.: 82 °C; FTIR (selected bands): 2960, 2872, 2176, 1474, 1350, 1241, 1078, 1031, 875, 681 cm$^{-1}$. Single crystals were obtained by seeding a quasi-saturated solution of **1** and **3b** (2 : 1 molar ratio) in methanol with the finely ground powder obtained from the solid-state synthesis, and then allowing for the slow evaporation of the solvent at room temperature.

## Results and discussion

### Polymorph screening

The crystal structure of **1** is unknown and it was expected that different polymorphs may be formed as several electron-donor sites, *i.e.*, oxygen, chlorine, and π-systems, can accept XB from the iodoalkyne moiety. Several crystallization conditions were thus employed in order to explore the structural landscape of **1** and obtain different polymorphic forms.

Slow evaporation of a chloroform solution of **1** afforded polymorph **1a** as octahedral crystals with m.p. of 111 °C. The single crystal X-ray analysis revealed that XB plays a role in the structure of **1a** (Fig. 1, top). In fact, the iodine atom

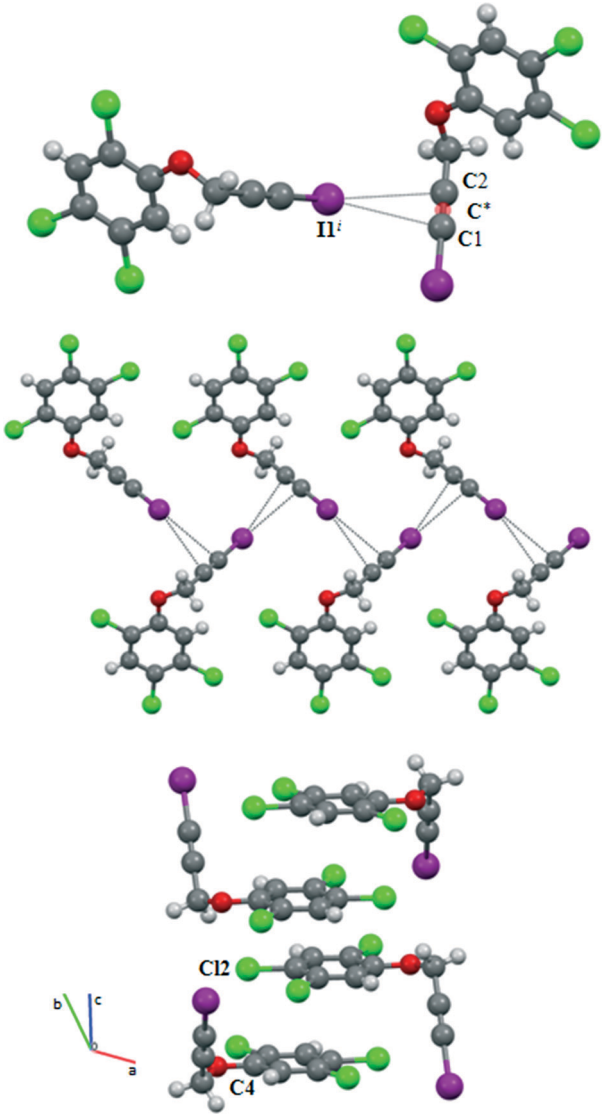


**Fig. 1** Top: XBs between the iodine atom and the π electrons of the triple bond in **1a**. Mid: supramolecular zigzag and halogen-bonded chain. Bottom: anti-parallel π–π stacking of **1** molecules involving the aromatic portions of two haloprogin molecules. XBs are black dotted lines. The triple bond centroid is indicated with a transparent red dot and the symbol C*. Colour code: carbon, grey; hydrogen, light grey; oxygen, red; chlorine, green; iodine, purple.

functions as the XB donor and forms a short contact with the π-electron density of the triple bond, working as the XB acceptor, of another molecule of haloprogin (symmetry operation 1/2 − *x*, 1/2 + *y*, 1/2 − *z*). An infinite halogen-bonded chain is formed and propagates parallel to the crystallographic *b* axis (Fig. 1, mid). The supramolecular chains of haloprogin molecules display a zig-zag arrangement with a I1···C*···I1$^{i}$ (*i* = 1/2 − *x*, 1/2 + *y*, 1/2 − *z*) angle of 85.2°, C* being the centroid of the triple bond. The C*···I1$^{i}$ distance is 3.556(3) Å (C2···I1$^{i}$ and C1···I1$^{i}$ distances are 3.560(3) Å and 3.649(3) Å, respectively), while the C1–I1···C* angle is 148.3(2)°. It should be noted here that these geometrical parameters are slightly longer and less linear than those found in similar supramolecular synthons reported in the CSD (see ESI†).[21] π–π Stacking interactions between couples of anti-parallel aromatic rings are also present with a separation of the ring centroids of 3.831 Å (Fig. 1, bottom).

Looking for other polymorphic forms of **1**, several organic solvents and their combinations were explored. All experiments resulted in the exclusive formation of polymorph **1a** (see ESI†) when the ionic strength of the crystallization medium was drastically increased. In fact, when a chloroform solution of haloprogin was allowed to slowly diffuse into a saturated methanol solution of sodium acetate and the resulting solvents mixture was slowly evaporated at room temperature (two days), some crystals of two new polymorphs, **1b** and **1c**, were obtained along with massive quantities of **1a**. Specifically, some rectangular needle-like crystals (**1b**, m.p. 113 °C) and a few long and tiny needles (**1c**, m.p. 91 °C) were formed together with larger amounts of **1a** (octahedral crystals, m.p. 111 °C). Interestingly, a similar mixed phase was also obtained by sublimating powders of **1a**.

Single crystal X-ray analyses demonstrated that **1a**, **1b**, and **1c** present quite different patterns of XBs. In polymorph **1b**, the iodine atom works as XB donor sites, similar to **1a**, but the XB acceptor site is the *para* positioned chlorine atom of its centrosymmetric molecule which presents the same XB pattern and a cyclic dimer is formed (Fig. 2, top left). The I···Cl distance is 3.633(2) Å (0.97% of the sum of van der Waals radii[22] (svdWr) of involved atoms) and the C–I···Cl and I···Cl–C angles are 171.71(9)° and 103.67(11)°, respectively.

These two angles are perfectly in line with the anisotropic electrostatic potentials around halogen atoms, with the iodine atom interacting through its electron poor σ-hole and the chlorine atom through its electron rich equatorial belt. Some other short contacts are present in this polymorph. Two HBs bridge two adjacent haloprogin molecules by connecting the chlorine atom of one molecule to one of the methylene hydrogens of another molecule ($H3_B$···Cl1 distance is 2.82 Å, 0.96% of svdWr

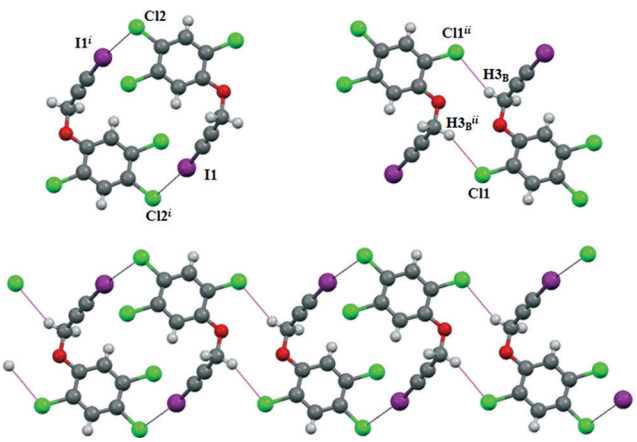


**Fig. 2** Structural motifs present in polymorph **1b**. "Head to tail" dimers originated by two I···Cl XBs (top left, XBs as black lines) and two H···Cl HBs (top right, HBs as magenta lines). Infinite chain formed by halogen and hydrogen bonds. Label of equivalent position: *i* (1 − *x*, 1 − *y*, 2 − *z*) and *ii* (1 − *x*, 1 − *y*, 1 − *z*). Colour code of atoms as in Fig. 1.

of involved atoms) and hydrogen-bonded cyclic dimers are formed (Fig. 2, top right). Halogen and hydrogen-bonded cyclic dimers are connected in the overall crystal packing of polymorph **1b** and produce ribbons extending along the *c*-axis (Fig. 2, bottom).

It seems that crystals of polymorph **1c** are quite unstable as, at room temperature, they convert into a powder sample of **1a**. As a consequence, the collection of a complete crystallographic data set was not possible but the obtained data were enough to refine the crystal structure and have essential structural information (Table 1). Similar to polymorphs **1a** and **1b**, the crystal structure of **1c** also presents XBs which are, here, the only noncovalent interactions below the svdWr of involved atoms. The iodine atom functions as a bifurcated XB donor and interacts both with the oxygen atom and with the chlorine atom *ortho* to the propargyl ether moiety (Fig. 3, left). The I1···Cl1$^{ii}$ (*ii* = 1 − *x*, 1 + *y*, 1/2 − *z*) distance is 3.442(4) Å (0.92 the svdWr of involved atoms) and the C1–I1···Cl1$^{ii}$ angle is 168.8(3)°, while the I1···O1$^{ii}$ distance is 3.448(10) Å (0.98 the svdWr of interacting atoms) and the C1–I1···O1$^{ii}$ angle is 141.7(4)°. These geometrical parameters closely resemble those reported in the literature for bifurcated XBs[23] where one XB contact is commonly shorter and more linear than the other. The propagation of this XB synthon results in infinite helical chains that develop along the *b* axis (Fig. 3, right).

Computational studies provided interesting pieces of information on the relative stabilities of the conformations adopted by molecule **1** in the three polymorphs. Molecule **1** has few degrees of conformational freedom which can be identified by the two torsion angles $\varphi_1$ (C3–O1–C4–C5) and $\varphi_2$ (C2–C3–O1–C4) (Scheme 1). The superposition of the aromatic rings of molecule **1** in the conformations adopted by the three obtained polymorphs shows how in **1a** and **1b** the molecular geometry is almost identical with the two torsion angles that are very similar to each other (Fig. 4, left).

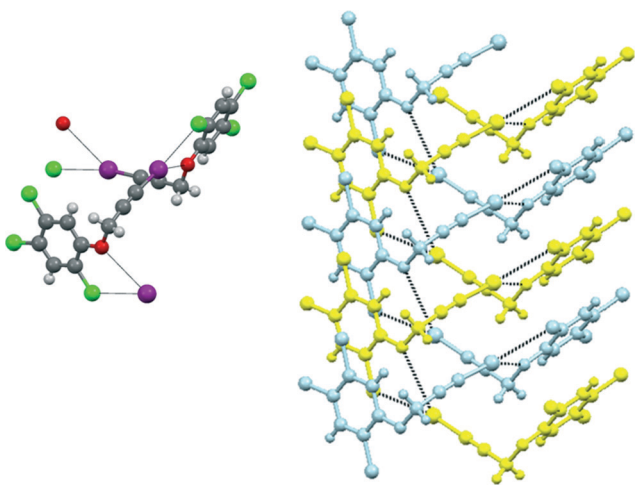

Fig. 3 Left: the bifurcated XB motif present in **1c**. Colour code as in Fig. 1. Right: two helical chains. Two different colours are used to highlight the different rotations of the chains.

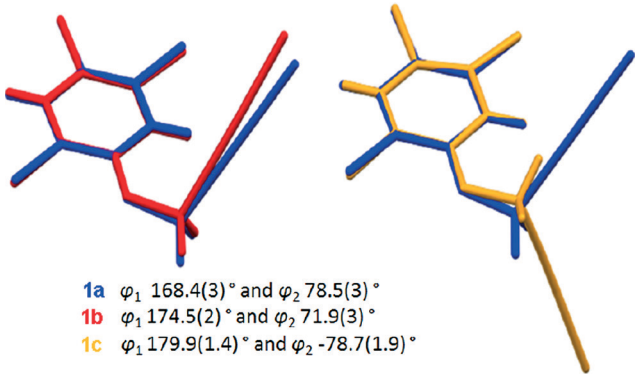


Fig. 4 Comparison of the molecule conformations of the three polymorphs **1a**–**c**. The torsion angles $\varphi_1$ and $\varphi_2$ are reported. Colour code: **1a**, blue; **1b**, red; and **1c**, yellow.

On the contrary, the haloprogin molecule in polymorph **1c** adopts a quite different conformation as shown in Fig. 4, right. Single point calculations (MP2/6-311+G(d,p)) on the X-ray molecular structures of the three polymorphs of haloprogin revealed that the conformation adopted in **1a** is the most stable (2.5 kJ mol$^{-1}$ more stable than **1b**) while the conformation of **1c** is the least stable (17.1 kJ mol$^{-1}$ less stable than **1a**).

These calculations and the similarity of the respective melting points may suggest that polymorphs **1a** and **1b** are energetically similar although their intermolecular networks are different. Polymorph **1a** is quasi-exclusively obtained in the crystallization experiments and this may suggest that, in spite of the fact that in any haloprogin molecule there are three chlorine atoms *versus* one triple bond, the I···π synthon is more favoured than the I···Cl one. Definitely, the polymorph **1c** is the least stable in the conditions used, as demonstrated by the small obtainable amount and by the fact that it converts into **1a** with time at room temperature.

## Co-crystal formation

Being the iodoalkynyl moiety a robust XB donor,[7–10] we decided to investigated the formation of co-crystals involving **1** and both neutral and anionic electron density donor partners. Here we describe the adducts **4** and **5a, b** obtained when 4,4′-bipyridine (**2**) and tetrabutylammonium iodide (**3a**) or chloride (**3b**) are used as XB acceptors.

Adduct **4** was obtained by slow evaporation of a 2 : 1 mixture of the two starting materials **1** and **2** dissolved in methanol. The DSC thermogram suggested the formation of a new supramolecular entity since it showed a single and sharp melting endotherm at 118 °C, *i.e.*, higher than the melting points of the starting compounds (**2** m.p. 109–112 °C). FTIR analysis confirmed that the supramolecular adduct formation involves the iodoalkynyl group, since the stretching band of the C≡C bond is at 2187 cm$^{-1}$ in **1a** and at 2178 cm$^{-1}$ in the adduct **4**. This red shift clearly indicates that the iodine atom is halogen-bonded to a strong electron density-donor site.[4]

The single crystal XRD analysis confirmed the formation of a 2 : 1 complex in which the molecule of **2** functions as a ditopic XB acceptor and interacts at each end with two distinct molecules of **1** thanks to I···N XBs (Fig. 5). The asymmetric unit is composed of two almost identical but independent XB donor molecules bound to the same bipyridine unit. Both the XBs are extremely short, linear, and similar in their geometrical parameters. I···N distances are 2.813(3) Å for I1A···N1 and 2.889(3) Å for I1B···N2 (around 80% reduction of the svdWr of the interacting atoms) and angles C1A–I1A···N1 and C1B–I1B···N2 are 177.95(10)° and 177.84(10)°, respectively.

The crystal lattice of adduct **4** is also stabilised by other noncovalent interactions, most relevant are the type-I halogen–halogen contacts occurring between two chlorine atoms [Cl3B···Cl3B$^{iii}$ (*iii* = $-x$, $1-y$, $1-z$), distance 3.320(2) Å and C8B–Cl3B···Cl3$^{iii}$ angle 127.77(10)°] and the π–π stacking between aromatic rings (with ring centroid separations of 3.597 Å).

The syntheses of co-crystals of **5a, b** were carried out *via* mechanochemical reactions between **1** and ammonium halides **3a, b**. Halide anions can work as polydentate XB acceptors and the number of formed interactions varies from one system to the other. DSC titration methods were used to determine the preferred pairing ratios between **1** and **3a, b**. DSC analyses of 1 : 1 and 3 : 1 mixtures of **1** and **3a** both showed multiple endothermic peaks. A new peak at 67 °C, mismatching the starting components, was shown by both mixture along with the melting of pure **3a** (at 141 °C) in the 1 : 1 mixture and of pure **1a** (at 111 °C) in the 3 : 1 mixture. This suggests that some excess starting component was present in both cases and that the preferred **1** : **3a** pairing ratio in **5a** is 2 : 1. Indeed, a mixture with this exact composition showed a single endothermic peak at 67 °C. A similar DSC analysis revealed that also the pairing ratio for complex **5b** (m.p. 83 °C) was 2 : 1.

FTIR spectroscopy on these halogen-bonded ionic co-crystals showed red-shifted triple bond stretching modes from 2187 cm$^{-1}$ in pure **1a** through 2180 cm$^{-1}$ in **5a** and to 2175 cm$^{-1}$ in **5b**, suggesting the involvement of the iodoalkynyl fragment in the co-crystal formation. The observed red-shift trend is also consistent with the chloride anion being a better XB acceptor than the iodide anion.

Very few good quality single crystals of **5a** and **5b** were obtained by adding finely ground powders of the complexes obtained from the mechanochemical syntheses to quasi-saturated methanol solutions of the starting compounds (2 : 1 molar ratio). Their single crystal structure determination confirmed the formation of a new supramolecular adduct composed of two molecules of haloprogin and one molecule of ammonium halide.

The asymmetric unit of **5a** is composed of one molecule of **1** and half molecule of **3a**, which lies on a twofold axis. The complex is assembled thanks to strong XBs occurring between the iodine atom of **1** and the iodide anion of the organic salt, which behaves as a bidentate XB acceptor (Fig. 6, left). The distance between the XB donor and acceptor is 3.3977(4) Å (82% reduction of the svdWr of I and the Pauling ionic radius of I$^-$) and the C1–I1···I2 angle is 175.73(12)°, both these values indicating the occurrence of a strong XB. The halide coordination sphere is completed by four HB contacts with H atoms belonging to the cation alkyl chains.

The crystal structure of **5b** (Fig. 6, right) is similar to **5a**. The chloride ion is halogen-bonded to iodine atom with a I1···Cl4 distance of 3.0427(5) Å (80% reduction of the svdWr of I and the Pauling ionic radius of Cl$^-$) and C1–I1···Cl4$^-$ angle of 176.00(4)° (Fig. 6, right). This remarkably short distance confirms that the C–I···Cl$^-$ synthon is stronger than the C–I···I$^-$ one, in good agreement with the differences in melting point and red-shift of triple bond stretching modes in FTIR spectra. In this case, the halide anion coordination sphere is completed by two HB interactions involving the hydrogen atoms of cation alkyl chains.

## Solid state NMR studies

Further characterization of the bulk materials was performed by multinuclear Solid State NMR studies (SSNMR). Different from HB,[24,25] only in recent years SSNMR has been applied to investigate XB.[26] This has been done mainly by analysing directly involved nuclei such as $^{19}$F, $^{14/15}$N, $^{35}$Cl, $^{81}$Br, and $^{127}$I,[27] but also neighbouring atoms have been considered.[28] For instance, it was shown that $^{13}$C resonances of halogen-bonded carbon atoms are broadened or even split due to a

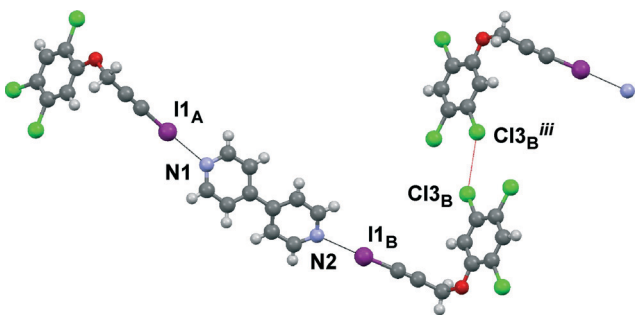


**Fig. 5** XBs (black dotted lines) and type I chlorine–chlorine interactions (red dotted lines) in co-crystal **4**. Label of equivalent position: *iii* ($-x$, $1-y$, $-z$). Colour code: blue, nitrogen; other colours as in Fig. 1.

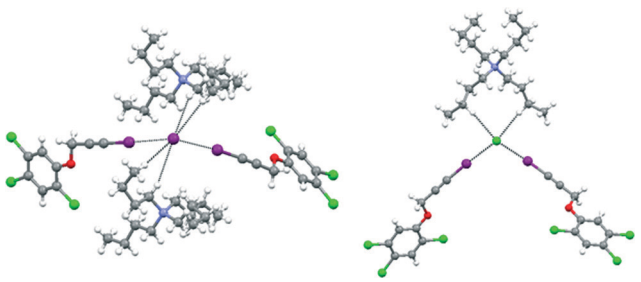

**Fig. 6** Bonding pattern around halide anions in the co-crystals **5a** (left) and **5b** (right). XBs and HBs are pictured as black dotted lines. In both **5a** and **5b** the N atom of the tetra-*n*-butylammonium cation lies on a twofold axis. Colour code as in Fig. 1.

$2^{nd}$ order effect of dipolar coupling to the quadrupolar $^{35/37}Cl$ (both spin 3/2) or $^{127}I$ (spin 5/2) nuclei,[29] thus confirming the proposed assignment for these signals.

Owing to the intrinsic difficulty of achieving relevant quantities of **1b** and **1c** polymorphs, here we report only the SSNMR characterization of **1a** and of the three co-crystals **4**, **5a**, and **5b**. The $^{13}C$ Cross Polarization Magic Angle Spinning (CPMAS) spectrum of **1a** is characterized by a broad resonance at 14.4 ppm assigned to C1 (Fig. 7). This carbon gives a signal at 6.97 ppm in $CDCl_3$ solution and at 18.58 ppm in $C_6D_5N$ solution, indicating that the C1 chemical shift moves upfield when the iodine atom is halogen-bonded.[4] The observed chemical shift in **1a** is in agreement with the presence of a XB between the iodine atom and the π electrons of the triple bond. While the details of the relationship between the XB strength and the upfield shift of C1 remains to be established, the small difference in the chemical shift of **1a** in the solid and in chloroform solution (where no, or negligibly weak, XBs are present) may suggest that the I···π electrons in **1a** is a medium-strength XB.

It is expected that the I···N XB, present in co-crystal **4**, is stronger than the I···π electrons XB, occurring in **1a**; and the C1 signal in crystalline **4** is at 25.1 ppm (Fig. 7). The presence of the I···N XB in this co-crystal is further confirmed by the $^{15}N$ (40.55 MHz) CPMAS spectra (see ESI†) showing that the pyridine nitrogen moves from 289.0 (in pure **2**) to 273.7 ppm (in co-crystal **4**).

As far as the SSNMR spectra of the ionic co-crystals **5a** and **5b** are concerned, the C1 signal is found at 31.6 and 33.0 ppm in **3a** and **3b** complexes, respectively (Fig. 7). These chemical shifts are consistent with the formation of C–I···$Y^-$ synthons (Y = I, Cl) and they may also suggest that chloride anions are better XB acceptors than the iodide anion and that halides are better XB acceptors than the neutral pyridine species.

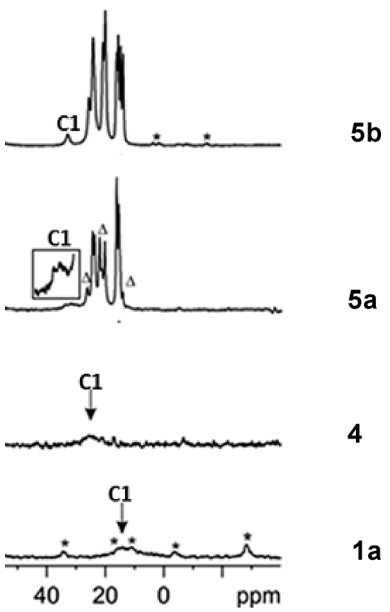


Fig. 7 $^{13}C$ (100.65 MHz) CPMAS spectra (region of the C1 resonance) of **1a** and co-crystals **4** and **5a, b** recorded at a spinning of 12/13 kHz. Asterisks and triangles mark spinning sidebands and unreacted **3a**.

## Conclusions

In summary, herein we have reported a polymorph screening and co-crystal formation study of the antifungal agent haloprogin (1,2,4-trichloro-5-[(3-iodoprop-2-yn-1-yl)oxy]benzene, **1**), a well-known halogenated API. We have described three polymorphs and three co-crystals involving both neutral and ionic CCFs. These are the first crystal structures reported in the CSD involving **1**.

In the described cases, the 1-iodoalkyne moiety has been shown to be a very effective XB donor. In the crystallization of pure haloprogin, the iodine atom probes the accessible electron donor sites and the three obtained polymorphs result from this sampling process, the iodine atom binding to the π-electrons of the triple bond (in **1a**), one chlorine atom (in **1b**), and one chlorine and oxygen atom (in **1c**). When more effective electron donor sites are made accessible by the presence of the CCFs **2** and **3a, b**, co-crystals are formed wherein the iodine atom binds to the pyridine nitrogen (in **4**) and the halide anions (in **5a, b**).

The obtained crystals have been fully characterized with various techniques (single crystal and powder X-ray crystallography, solid state NMR, IR, and DSC), which have all shown that XB is a key interaction responsible for the adopted architectures in the described systems. The strategy reported in this paper is general and may find wide application in the design of new pharmaceutical polymorphs and co-crystals involving halogenated active pharmaceutical ingredients.

## Acknowledgements

P.M., G.R., and G.T. thank Fondazione Cariplo (grant number 2010-1351) and MIUR (projects PRIN 2010–2011, grant numbers 2010CX2TLM_004 and 2010ERFKXL_005) for financial support.

## Notes and references

1 (*a*) W. Jones, W. D. S. Motherwell and A. V. Trask, *MRS Bull.*, 2006, **31**, 875; (*b*) P. Vishweshwar, J. A. McMahon, J. A. Bis and M. J. Zaworotko, *J. Pharm. Sci.*, 2006, **95**, 499; (*c*) N. Issa, P. G. Karamertzanis, G. W. Welch and S. L. Price, *Cryst. Growth Des.*, 2009, **9**, 442; (*d*) C. B. Aakeröy, S. Forbes and J. Desper, *J. Am. Chem. Soc.*, 2009, **131**, 17048; (*e*) C. B. Aakeröy, A. B. Grommet and J. Desper, *Pharmaceutics*, 2011, **3**, 601; (*f*) D. R. Weyna, M. L. Cheney, N. Shan, M. Hanna, Ł. Wojtas and M. J. Zaworotko, *CrystEngComm*, 2012, **14**, 2377; (*g*) F. L. F. Soares and R. L. Carneiro, *Cryst. Growth Des.*, 2013, **13**, 1510.

2 A. Lemmerer and J. Bernstein, *J. Chem. Crystallogr.*, 2011, **41**, 991.

3 A halogen bond occurs when there is evidence of a net attractive interaction between an electrophilic region associated with a halogen atom in a molecular entity and a nucleophilic region in another, or the same, molecular entity. G. R. Desiraju, P. S. Ho, L. Kloo, A. C. Legon, R. Marquardt, P. Metrangolo, P. Politzer, G. Resnati and K. Rissanen, *Pure Appl. Chem.*, 2013, **85**, 1711.

4 M. Baldrighi, G. Cavallo, M. R. Chierotti, R. Gobetto, P. Metrangolo, T. Pilati, G. Resnati and G. Terraneo, *Mol. Pharmaceutics*, 2013, **10**, 1760.

5 (*a*) E. F. Harrison, P. Zwadyk, R. J. Bequette, E. E. Hamlow, P. A. Tavormina and W. A. Zygmunt, *Appl. Microbiol.*, 1970, **19**, 746; (*b*) E. F. Harrison and W. A. Zygmunt, *Can. J. Microbiol.*, 1974, **20**, 1241; (*c*) E. Gregori-Puigjané, V. Setola, J. Hert, B. A. Crews, J. J. Irwin, E. Lounkine, L. Marnett, B. L. Roth and B. K. Shoichet, *Proc. Natl. Acad. Sci. U. S. A.*, 2012, **109**, 11178; (*d*) G. Stuettgen, J. Mueller and W. Roelz, *Antimycotic preparations in a cream or ointment base*, GB2116425A, 1983; (*e*) I. R. McGraw, *Use of Haloprogin to treat Herpes Labialis*, US4434183, 1984; (*f*) J. Ponikau, *Use of antifungal agents for the topical treatment of fungus-induced mucositis*, EP1024814, 2007.

6 F. H. Allen, *Acta Crystallogr., Sect. B: Struct. Sci.*, 2002, **58**, 380.

7 C. B. Aakeröy, M. Baldrighi, J. Desper, P. Metrangolo and G. Resnati, *Chem. – Eur. J.*, 2013, **19**, 16240.

8 T. Clark, M. Hennemann, J. S. Murray and P. Politzer, *J. Mol. Model.*, 2007, **13**, 291.

9 (*a*) P. Metrangolo, F. Meyer, T. Pilati, G. Resnati and G. Terraneo, *Angew. Chem., Int. Ed.*, 2008, **47**, 6114; (*b*) M. Fourmigué, *Curr. Opin. Solid State Mater. Sci.*, 2009, **13**, 36; (*c*) T. M. Beale, M. G. Chudzinski, M. G. Sarwar and M. S. Taylor, *Chem. Soc. Rev.*, 2012, **42**, 1667; (*d*) M. Erdélyi, *Chem. Soc. Rev.*, 2012, **41**, 3547; (*e*) F. Meyer and P. Dubois, *CrystEngComm*, 2013, **15**, 3058; (*f*) G. Cavallo, A. Priimagi, P. Metrangolo and G. Resnati, *Acc. Chem. Res.*, 2013, **46**, 2686; (*g*) R. W. Troff, T. Makela, F. Topic, A. Valkonen, K. Raatikainen and K. Rissanen, *Eur. J. Org. Chem.*, 2013, **9**, 1617.

10 C. Perkins, S. Libri, H. Adams and L. Brammer, *CrystEngComm*, 2012, **14**, 3033.

11 D. Braga, F. Grepioni, L. Maini, D. Capucci, S. Nanna, J. Wouters, L. Aerts and L. Quéré, *Chem. Commun.*, 2012, **48**, 8219.

12 GRAS (Generally Recognized As Safe) Notices: http://www.cfsan.fda.gov/~rdb/opa-gras.html.

13 J. Fellig, J. R. Barnes, A. I. Rachlin, J. P. O'Brien and A. Focella, *J. Agric. Food Chem*, 1970, **18**, 78.

14 *Saint Plus, v.6.01*, Bruker Analytical X-ray, Madison, WI, 1999.

15 (*a*) G. M. Sheldrick, *SADABS: Empirical Absorption Correction Program*, University of Gottingen, Germany, 2001. Based upon the method of Blessing; (*b*) R. H. Blessing, *Acta Crystallogr., Sect. A: Found. Crystallogr.*, 1995, **51**, 33.

16 *APEXII v2009. 5–1*, © 2009, Bruker Analytical X-ray Systems, Madison, WI.

17 G. M. Sheldrick, *Acta Crystallogr., Sect. A: Found. Crystallogr.*, 2008, **64**, 112.

18 L. J. Farrugia, *J. Appl. Crystallogr.*, 1999, **32**, 837.

19 *Mercury 3.1*, © CCDC 2001–2012.

20 *Spartan'10*, Wavefunction Inc., Irvine, CA.

21 C. J. Adams and L. E. Bowen, *Dalton Trans.*, 2005, 2239; T. Graening, V. Bette, J. Neudorfl, J. Lex and H.-G. Schmalz, *Org. Lett.*, 2005, **7**, 4317; A.-L. Barres, A. El-Ghayoury, L. V. Zorina, E. Canadell, P. Auban-Senzier and P. Batail, *Chem. Commun.*, 2008, 2194.

22 A. Bondi, *J. Phys. Chem.*, 1964, **68**, 441.

23 (*a*) A. B. Sheremetev, J. L. Shamshina, D. E. Dmitriev, D. V. Lyubetskii and M. Y. Antipin, *Heteroat. Chem.*, 2004, **15**, 199; (*b*) L. Ouahab, F. Setifi, S. Golhen, T. Imakubo, R. Lescouezec, F. Lloret, M. Julve and R. Swietlik, *C. R. Chim.*, 2005, **8**, 1286; (*c*) K. D. Scherfise, F. Weller and K. Dehnicke, *Z. Naturforsch., B: J. Chem. Sci.*, 1985, **40**, 906.

24 (*a*) M. R. Chierotti and R. Gobetto, *Chem. Commun.*, 2008, 1621; (*b*) S. P. Brown, *Solid State Nucl. Magn. Reson.*, 2012, **41**, 1; (*c*) X. Filip, I. G. Grosu, M. Miclaus and C. Filip, *CrystEngComm*, 2013, **15**, 4131.

25 (*a*) J. P. Bradley, C. J. Pickard, J. C. Burley, D. R. Martin, L. P. Hughes, S. D. Cosgrove and S. P. Brown, *J. Pharm. Sci.*, 2012, **101**, 1821; (*b*) M. U. Schmidt, J. Bruning, J. Glinnemann, M. W. Hutzler, P. Morschel, S. N. Ivashevskaya, J. van de Streek, D. Braga, L. Maini, M. R. Chierotti and R. Gobetto, *Angew. Chem., Int. Ed.*, 2011, **50**, 7924.

26 (*a*) C. M. Widdifield, G. Cavallo, G. A. Facey, T. Pilati, J. Lin, P. Metrangolo, G. Resnati and D. L. Bryce, *Chem. – Eur. J.*, 2013, **19**, 11949; (*b*) J. Viger-Gravel, S. Leclerc, I. Korobkov and D. L. Bryce, *CrystEngComm*, 2013, **15**, 3168.

27 (*a*) R. J. Attrell, C. M. Widdifield, I. Korobkov and D. L. Bryce, *Cryst. Growth Des.*, 2012, **12**, 1641; (*b*) J. Viger-Gravel, I. Korobkov and D. L. Bryce, *Cryst. Growth Des.*, 2011, **11**, 4984; (*c*) M. G. Chudzinski, C. A. McClary and M. S. Taylor, *J. Am. Chem. Soc.*, 2011, **133**, 10559.

28 (*a*) Nonappa, M. Lahtinen, E. Kolehmainen, J. Haarala and A. Shevchenko, *Cryst. Growth Des.*, 2013, **13**, 346; (*b*) C. Lemouchi, C. S. Vogelsberg, L. Zorina, S. Simonov, P. Batail, S. Brown and M. A. Garcia-Garibay, *J. Am. Chem. Soc.*, 2011, **133**, 6371.

29 C. Pettinari, C. Di Nicola, F. Marchetti, R. Pettinari, B. W. Skelton, N. Somers, A. H. White, W. T. Robinson, M. R. Chierotti, R. Gobetto and C. Nervi, *Eur. J. Inorg. Chem.*, 2008, 1974.